Food Bioprocess Technol (2014) 7:2423–2433
DOI 10.1007/s11947-014-1305-y

ORIGINAL PAPER

Physicochemical and Engineering Properties of Nanocomposite Films Based on Chitosan and Pseudoboehmite Alumina

T. A. Shittu · J. Jayaramudu · D. Sivakumar · E. R. Sadiku

Received: 3 August 2013 / Accepted: 18 March 2014 / Published online: 22 April 2014

Abstract Chitosan-based nanocomposite plastic films were developed by adding 0, 1, 3, and 5 % boehmite alumina (BAH) nanoparticles as a percentage of chitosan powder weight. The films were cast via solution. The effect of BAH content on the physicochemical and engineering properties of the resultant films were determined. The swelling, water vapor adsorption capacity, and transparency were significantly reduced with increased BAH content. The stability of the films against microbial degradation under high relative humidity also increased with BAH content. The water vapor permeability (WVP) reduced with increased temperature giving rise to negative activation energy values, which ranged between 2.08 and 3.36 kJ/mol. However, at constant temperature, inclusion of BAH did not have significant effect on water vapor permeability (WVP). WVP was predicted to high accuracy (r^2= 0.984) using a full quadratic regression model. All the films had similar tensile and thermal behaviors. The implications of the findings are discussed based on prospective applications of the biodegradable film especially for fresh produce packaging.

Keywords Chitosan · Alumina · Nanocomposite film · Engineering properties · Water vapor permeability

T. A. Shittu · D. Sivakumar
Postharvest Technology Group, Department of Crop Sciences, Tshwane University of Technology, Pretoria 0001, South Africa

J. Jayaramudu · E. R. Sadiku
Polymer Technology Division, Department of Chemical, Metallurgical and Materials Engineering, Tshwane University of Technology, Pretoria 0001, South Africa

T. A. Shittu (✉)
Department of Food Science and Technology, Federal University of Agriculture, Abeokuta 110001, Nigeria
e-mail: staofeek0904@yahoo.com

Introduction

The increasing packaging requirements of the food industry have engendered several studies that involve the design and development of appropriate packaging materials capable of providing additional function apart from the primary functions of protecting, displaying, and unitizing products. The other central issue in the packaging and food industry is that of environmental friendliness in terms of recyclability and biodegradability of packaging material (Subramanian 2000). This has necessitated the search for biodegradable polymer materials that can replace nondegradable synthetic organic compounds such as polyethylene, polystyrene, etc. which have been used for many years in the industries (Aminabhavi et al. 1990). Due to the diverse nature of biopolymers, extra efforts are required to modify them to have suitable functional properties (mechanical, barrier, optical, and thermal) for various practical applications.

Chitosan, deacetylated chitin polysaccharide, is a major constituent of the exoskeleton of crustaceans. It has high molecular weight and dissolves in acidic aqueous media to form gels, films, and fibers (Hirano et al. 1999; Ghanem and Skonberg 2002). Due to its cationic nature, chitosan has some antimicrobial and functional properties. The functional properties of its solutions and dried films depend on the degree of acetylation and molecular weight. Chitosan film thickness and flexibility have also been reported to increase with increased molecular weight of the acid used for acetylation (Begin and Van Calsteren 1999). Park et al. (2002) reported that higher molecular weight of chitosan increased the mechanical strength but had no significant effect on water vapor permeability of the films. Butler et al. (1996) and Caner et al. (1998) reported that chitosan films have good barrier properties to oxygen, while having low water vapor barrier properties because of their hydrophilic nature. The high permeability to water vapor is a great limitation to many of their uses but may

be of advantage in some other applications. Another advantage of chitosan as a polymer for making packaging materials is that it gives transparent films. However, the film's transparency could vary with the composition of the film forming solution (Leceta et al. 2013) and drying method (Srinivasa et al. 2004).

The application of organic polymers, metallic and nonmetallic oxide nanoparticles, and their blends or derivatives in order to modify the functional properties of biopolymeric films is well documented. The nanoparticles, as opposed to organic polymers, are often added in minute quantities to effect the functional modifications. Addition of EDTA (Singh et al. 2012), poly-(ε-caprolactone) (Swapna et al. 2011), silicate or clays (Bhunia et al. 2012; Avella et al. 2007), ZnO (Bajpai et al. 2012), TiO_2 (Schutz et al. 2012), AgO and ZnO (Emamifar et al. 2010) to different polymeric film forming solutions (FFS) resulted in modification of film's barrier, thermal, mechanical, and optical properties. The metallic nanomaterials were also reported to impart efficient antimicrobial properties to the nanocomposite packaging materials developed (Tayel et al. 2011; Tripathi et al. 2011). In spite of the reported antimicrobial activity of alumina (Al_2O_3) nanoparticles against human and foodborne pathogens for clinical application (Amitava et al. 2011), studies on its potential applications in packaging materials are scarce. Recently, Ogunniran et al. (2012) reported significant improvement in the thermal and mechanical behaviors of graft of polypropylene/maleic anhydride with the addition of boehmite alumina (BAH), which is a precursor of Al_2O_3. Chen et al. (2008) also reported improved crack toughness of a transparent composite coating film when BAH was added up to 40 % of the formulation. They attributed this performance to the high aspect ratio of the BAH nanorods. To our knowledge, the use of BAH or pseudoboehmite in biopolymeric films has not been reported so far.

In this study, the effect of BAH addition to prepare chitosan film at some concentrations on the physical, chemical, thermal, optical, and water vapor permeability properties was investigated. The prospective use of the new nanocomposite films was discussed in the light of the findings.

Materials and Methods

Materials

Medium molecular weight chitosan powder (200–800 cP) and glacial acetic acid were obtained from Sigma-Aldrich (South Africa). The AlO(OH) powder used was a commercial product manufactured by Sasol (Hamburg, Germany), under the trade name Disperal40 containing 80 % Al_2O_3. The average particle size was 17 nm.

Film Forming Solution

The film forming solution was prepared by first adding ~2 mL acetic acid to 100 mL of distilled water at 23 °C in a 250-mL beaker with continuous stirring using a magnetic stirrer. Later, the BAH powder was dispersed in the aqueous phase to make 1, 3, and 5 % (*w*/*w*) concentrations, based on chitosan powder weight. Finally, about 2 g of chitosan powder was gradually added with continuous stirring for about 18 h in order to form homogenous viscous solution. The thick solution was thinly spread on a rectangular glass plate (35×20 cm). The film spread uniformity on the glass surface was maintained by spreading with a glass rod suspended at 0.3 cm above the glass surface. The film was then dried at room conditions (26 ±4 °C, 75–82 % RH) between 2–3 days depending on the ambient room temperature and relative humidity. Thereafter, the films were carefully peeled and kept at the same room conditions.

Moisture Content

About 0.4 g of the film was weighed using a digital balance (RADWAG Wagi Electronic-znc, Poland) with an accuracy of ±0.0001 g. The sample was then dried in an oven at 80 °C until the weight differences between three consecutive weights were equal or less than 0.0002 g. Analyses were done in triplicate.

Thickness and Density

The thickness of the composite films was determined using a micrometer screw gauge (0.01 mm accuracy) at eight different points on each sample of film. A total of four films (600–700 cm^2) were analyzed from every formulation. To determine the density, smaller film samples (4×4 cm^2) were cut, and their weights were determined to the nearest 0.0001 g. Film density was calculated as the weight divided by the area times the average thickness.

Swelling Capacity and Water Solubility

Square samples of the film of about 16 cm^2 were first dried in the oven at 80 °C for 48 h in order to determine the initial dry matter of the films (W_0). The film samples were then immersed in 50 mL distilled water at 22 °C for 24 h with intermittent agitation. Soaked samples were carefully removed and blotted with adsorbent nonshredding towel in order to remove the superficial water. Then, the weight was taken (W_1). The sample was later dried in an oven at 85 °C to a constant weight (W_2). Analyses were done in triplicate. The swelling capacity (SWC) was calculated by weight difference as described in Kim et al. (2006):

$$\mathrm{SWC}(\%) = 100 \times \left(\frac{W_1 - W_0}{W_0}\right) \quad (1)$$

Water solubility (WS) was also calculated as described in Khan et al. (2012):

$$\mathrm{WS} = 100 \times \left(\frac{\mathrm{W}_0 - \mathrm{W}_2}{\mathrm{W}_0}\right) \quad (2)$$

Total Titratable Acidity and pH

Dried samples (4×4 cm) were soaked in distilled water at 22 °C for 24 h, as described above, with intermittent agitation to extract solubles. About 10 mL of the soak water was titrated against 0.01 N NaOH solution using phenolphthalein as indicator. The acidity was calculated using acetic acid equivalence. The pH of the extract was determined with a digital pH meter (BT 500, BOECO, Germany). On each film sample, triplicate analyses were conducted.

Water Vapor Adsorption Capacity and Physical Stability

Preliminary experiment has shown that the film samples lose weight when exposed to high RH (>85 %) and temperature (>28 °C) conditions for times exceeding 24 h. Therefore, to prevent degradation, the film samples (4×4 cm) were placed in Petri dishes supported on wire gauze inside glass jars. The air in the glass jars was maintained at 22 °C and 95 % RH using glycerol solution (Forney and Brandl 1992). The initial (W_i) and final weights (W_f) of the film samples were taken to the nearest 0.0001 g. Water vapor adsorption capacity (WVAC) was calculated as:

$$\mathrm{WVAC}(\%) = 100 \times \left(\frac{W_f - W_i}{W_i}\right) \quad (3)$$

The film stability was determined by placing the samples in controlled relative humidity as described above, but the temperature was maintained at 35 °C. The sample weights were monitored for about 146 h. Change in weight was calculated as a percentage of the original weight. Triplicate analyses were done.

Water Vapor Permeability

The water vapor permeability (WVP) of the films was determined gravimetrically. Square films (4,900 mm^2) were first dried to constant weight in desiccators at 22 °C for 5 days over silica gel. The permeation cups used were made of glass with internal diameter and height of 40 and 65 mm, respectively. The cups were filled with saturated solution of lithium chloride in order to provide the relative humidity of 11.1–11.3 % at the test temperature used (12, 22, and 35 °C) to simulate the ambient temperatures in the temperate, tropical, and subtropical conditions. The cups were sealed with films using silicone. The films were held tightly to the glass cell with screw cap and then placed in a humidified and thermostatically controlled chamber to maintain the set temperatures. Weight gain of the cups was measured at intervals depending on the temperature used. The slope of weight loss vs. time (*g*/*s*) was obtained by linear regression. The WVP was then calculated as follows:

$$\mathrm{WVP} = \frac{x \cdot \mathrm{Slope}}{\Delta P \cdot A} \quad (4)$$

x is the film thickness (m), ΔP is the pressure difference (Pa) between the inside and outside of the cup, and A is the permeation surface area of film (m^2). The experiment was done in duplicate.

Color

The color parameters (L^*, a^*, b^*, chroma, and hue) of the films were determined using a Minolta Chroma Meter CR-400 (Minolta Camera Co Ltd, Japan) against a white background (L^*=93.86, a^*=−0.08, b^*=2.93) according to Leceta et al. (2013). Measurements were made at eight different points on every film with surface area of 465–600 cm^2. Quadruplicate sample of film was analyzed.

Light Transmission Property

The light transmission property of the films (thickness= 0.021–0.026 mm) was determined using ASTM D 1746-88 method (ASTM 2009). A UV-visible spectrophotometer (Model UVD-3000, Labomed Inc., USA) was used to determine the specular transmittance (T_s) through the film at 560 nm. Six replicates of film were analyzed. Film transparency was calculated as:

$$T_s(\%) = 100 * \left(\frac{T_f}{T_b}\right)$$

T_f and T_b are the light transmittance with and without the film.

Microstructural Analysis

Samples were cryogenically fractured (in liquid nitrogen), mounted on double-sided carbon tapes, and the fractured surfaces were coated with iridium (~5-nm thickness). Iridium coating has been reported to provide more effective charge

injection on film surface. The use of iridium oxide coating has been emphasized in Mailley et al. (2000). Samples were exposed to an accelerating voltage of 10 kV in a field emission scanning electron microscope (JSM-7600 F, JEOL Ltd., Tokyo, Japan).

About 280×300 pixel^2 size of each surface micrograph was cropped and analyzed to determine the surface characteristics of the films. The gray level matrix of the cropped surface images was presented in 3D. The analysis was done using ImageJ 1.45s software (National Institute of Health, USA). Analyses were done in duplicate.

Tensile Properties

The tensile properties of the films were determined according to ASTM D 882–02 standard (ASTM 1995). The parameters determined include tensile strength, modulus of elasticity, and % elongation at break with INSTRON 3369 Universal Testing Machine (Norwood, MA). Specimens were cut into rectangular shape with dimensions of 10×3.1×0.6 mm. The universal tester was run at a cross-head speed of 20 mm/min maintaining a gauge length of 50 mm and load cell capacity of 50 kN (11,250 lbf). All measurements were taken at 23 °C. Eight measurements were taken per sample, and the average values were reported.

Differential Scanning Calorimetry

The DSC analysis was done using PerkinElmer DSC 7 calibrated with nitrogen as standard. ASTM E-967 (ASTM 2008a) and ASTM E-968 methods (ASTM 2008b) were followed in temperature and heat calibration, respectively. Approximately 1 mg of the film was pre-dried over silica gel and placed in aluminum pans. The heating and cooling of sample were done from 30 to 300 °C at 10 °C/min and from 300 to 30 °C at 40 °C/min, respectively. The parameters measured include the onset (T_o) and peak of melting transition (T_p), enthalpy of melting, and glass transition temperature (T_g).

Data Analysis

Analysis of variance was done in order to explore the significance of mean differences, and the mean separation was done using Duncan's multiple range test (DMRT). The influence of temperature on the WVP was modeled using Arrhenius equation:

$$\mathrm{WVP} = \mathrm{WVP_o}\exp\left(\frac{-E_a}{\mathrm{RT}}\right) \tag{6}$$

$\mathrm{WVP_o}$ is the pre-exponential constant of WVP, E_a is the activation energy of permeation (kJ/mol), R is universal gas constant (8.314 J/mol/K), and T is the absolute temperature (K) of water vapor.

The experiment on WVP was based on two factors The response surface regression model for predicting the water vapor permeability value from the air temperature and BAH content was generated using Essential Regression (ER) which is a free add-in package for Excel (Available at: http://www.jowerner.homepage.t-online.de/download.htm).

Results and Discussion

Moisture content is an important property of any polymeric film as it affects the mechanical and handling behavior when used as packaging materials. Apart from the drying process, it has been reported that the type and amount of additive used affect the sorption/desorption behavior of biopolymeric film (Rodrıguez et al. 2006; Srinivasa et al. 2007a) which in turn affect the moisture content variation during use. It is required that the film should be drier than the product or it should have low moisture adsorption capacity when used for packaging of dried food and vice versa. Moisture content of the nanocomposite films obtained here did not differ significantly (Table 1). This might be due to the similar drying behavior of the film forming solution (FFS) regardless of their composition. Leceta et al. (2013) however reported higher moisture contents (15.70–21.57 %) for certain chitosan-based films which could be probably due to different drying conditions and composition of the FFS used.

It has been shown that water solubility of food packaging films affects its barrier properties (Mchugh et al. 1994). Water solubility is a measure of the film's resistance to water vapor transportation when used for packaging wet food products or when the film is used as food protective against humid environment (Bourtoom & Chinnan, 2008). Thus, higher solubility implies lower resistance. This property is particularly critical for fruit and vegetable packaging application because of the constant respiration and condensation of respiratory water vapor on the internal film surface when stored under low temperature. In this study, the solubility of the films significantly increased from 4.80 to 9.35 % with BAH content. The relationship is exponential as shown in Eq. 7. The values are lower than those reported by Leceta et al. (2013) even for films made from pure and low molecular weight chitosan powder. These authors also showed that solubility of chitosan-based films decreased with increased molecular weight of chitosan and heat treatment applied (Leceta et al. 2013). In this study, medium molecular weight chitosan was used. Hence, the increased solubility of the chitosan-BAH nanocomposite film with increased BAH could only be attributed to the hydrophilic nature of BAH (Chen et al. 2008). Abdollahi et al. (2012) reported an opposite effect when nanoclay was used as fillers. The lower solubility of the

Table 1 Some physicochemical, optical, and mechanical properties of chitosan nanocomposite films loaded with BAH nanoparticles

BAH content (%)	Moisture content (%)	Swelling index	Total Acidity (%, 10^{-3})	pH	WVAC (%)	Transparency (%)	L^*	a^*	b^*	ME (MPa)	ε (%)	TS (MPa)
0	9.38 (0.16)	3.86^{a} (0.94)	2.00 (0.65)	4.33 (0.17)	55.68^{a} (2.78)	88.55^{a} (0.87)	93.21^{a} (0.01)	-0.32^{a} (0.01)	3.89^{c} (0.09)	1097.1 (378.0)	8.2 (2.6)	8.2 (2.6)
1	9.36 (0.55)	1.65^{b} (0.01)	1.71 (0.16)	4.35 (0.04)	51.58^{c} (6.26)	84.59^{b} (2.24)	93.10^{a} (0.08)	-0.40^{ab} (0.01)	4.16^{bc} (0.09)	827.9 (292.5)	9.2 (3.1)	9.2 (3.1)
3	9.23 (1.36)	1.60^{b} (0.11)	1.65 (0.15)	4.35 (0.10)	53.86^{b} (2.79)	77.60^{c} (2.60)	93.03^{ab} (0.06)	-0.45^{b} (0.02)	4.58^{ab} (0.13)	1058.8 (391.8)	8.0 (1.0)	8.0 (1.0)
5	10.25 (0.43)	2.01^{b} (0.24)	1.29 (0.74)	4.37 (0.06)	54.47^{ab} (3.73)	71.06^{d} (1.19)	92.86^{b} (0.25)	-0.51^{b} (0.15)	4.99^{a} (0.62)	852.5 (138.1)	10.7 (3.0)	10.7 (3.0)

Means followed by different superscript are significantly different at $p<0.05$

ME modulus of elasticity, ε elongation, *TS* tensile strength

Values in parentheses are standard deviations of means

nanocomposite films obtained in this study compared to other reported chitosan-based films (Zivanovic et al. 2007; Leceta et al. 2013) makes them more suitable for wet food packaging applications.

$$\text{Solubility}\ (\%) = 4.60 \cdot e^{(0.1294 \cdot \text{BAH})} \quad \left(r^2 = 0.9358, p < 0.05\right) (7)$$

Swelling is a form of temporary microstructure modification mainly due to absorption of water or liquid molecule into the polymer matrix. It is an important property that determines the stability of the film during use when kept in wet condition. High polymer swelling is of immense benefit in biomedical application because it enhances water and/or bioactive compound absorption without dissolution. It permits gradual drug release due to the reduction of the free volume in polymer matrix and thus reduces molecular diffusion. The major disadvantage of swelling in the packaging industry is that it could negatively affect the mechanical strength of the film (Ulbricht 2006). The swelling capacity of the nanocomposite films prepared was significantly reduced with 1 % BAH addition when compared with neat chitosan (Table 1). Thereafter, additional BAH inclusion did not produce any difference in swelling of the film. This implies that the mechanical stability of the composite films in wet condition may be better than that of neat chitosan film. This hypothesis needs to be confirmed in a separate study.

The result as shown in Table 1 indicates that addition of BAH caused significant reduction in water vapor adsorption capacity of the films at 22 °C. This probably might be due to reduction of the adsorptive sites in the chitosan molecules with increased BAH binding thereby resulting in reduced wetting properties. The reduced water vapor adsorption capacity would be of great advantage especially when the films are used as wrapper in highly humid conditions as it is found in fruit and vegetable packaging and storage.

Higher BAH content also resulted in increased density of the films. This might be due to higher density of BAH (0.4–0.6 g/cm^3) as compared to that of chitosan (0.15–0.30 g/cm^3). The variation was linear as shown in Eq. 8. This variation in the bulk density could have significant effect on the mechanical and handling properties of the nanocomposite films.

$$\sigma = \ 0.0905 \cdot \text{BAH} + 0.8971 \quad \left(r^2 = 0.9215, p < 0.05\right) (8)$$

Although the acidity reduced with increased BAH (Table 1), the values were not significantly different. Similarly, the pH of the films did not differ. The acidity of the films is due to the residue of the acetic acid added while preparing the FFS. Therefore, the reducing acidity could have been caused by the higher extent of neutralization reaction with increasing concentration of the alkaline BAH.

Figure 1 indicates the weight changes of chitosan-based films when kept at very high humidity condition (RH=95 %). All the films gained weight after 20 h of exposure as a result of moisture adsorption. After 44 h of exposure, neat chitosan film had the highest weight gain followed by the 5 % BAH composite film. Nanocomposite film with 1 % BAH showed the highest initial weight gain, and it also showed the earliest

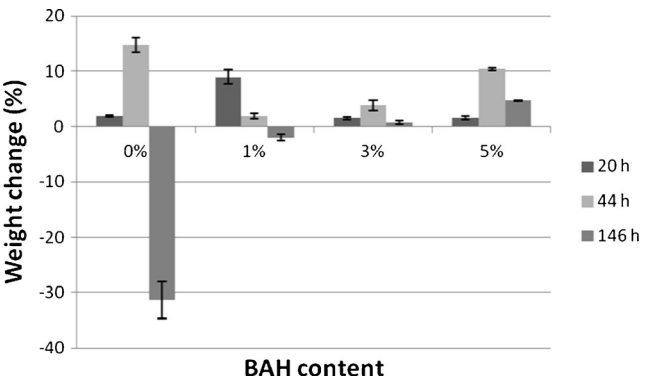

Fig. 1 Weight loss of chitosan-based films at 95 % RH for various storage times (potentially related to microbial degradation activity)

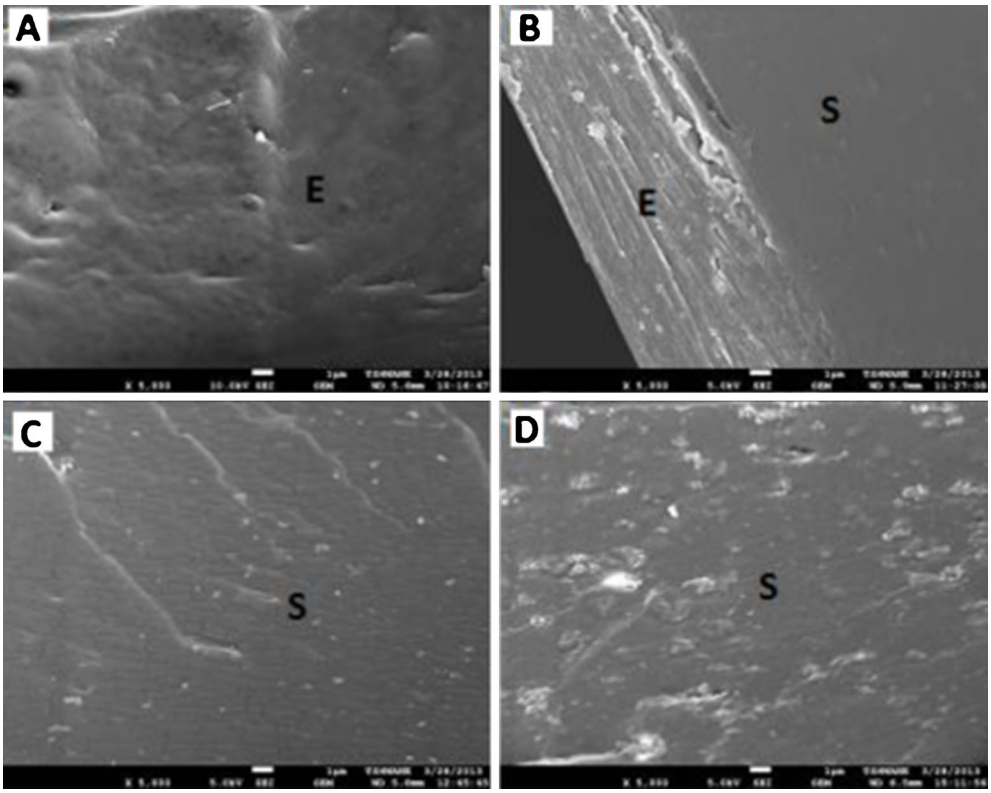

Fig. 2 Scanning electron micrograph of the edge (E) and the surface (S) of the chitosan-based films as affected by BAH content [A 0 %, B 1 %, C 3 %, D 5 %]. Magnification is ×5,000

sign of weight loss after 20 h. Other films lost weight after 44 h. The weight loss under such high water activity condition is attributed to microbial degradation of the film. Biodegradation of materials is preceded by either direct enzymatic or oxidative cleavage of the macromolecules giving rise to metabolizable fragments. The chain fragments become short enough to be converted by microorganisms (Stevens 2003). The films' biodegradability could have been reduced probably due to the increasing antimicrobial activity of films as a result of higher BAH content.

Table 1 shows the optical properties of the packaging films as affected by the BAH content. Varying the nanoparticles content significantly affected the optical properties ($p<0.05$). Transparency reduced with increased BAH content. The difference in transparency could not have been contributed by film thickness since they have similar thickness (mean=0.021, coefficient of variation=6.15 %). Transparency is important to packaging film for two main reasons. Firstly, it determines the exposure of packaged food material to the environmental light irradiation which could affect product quality positively or negatively over a prolonged storage period. Secondly, high transparency is, however, desirable for product sensory appreciation by consumers in retail outlets. However, some authors have reported that exposure of fruits and vegetables to UV light increased content of bioactive compounds (Bakhshi and Arakawa 2006; Xu et al. 2010) but accelerates ripening thereby reducing product's shelf life. Thus, reducing transparency with increased BAH content would make this nanocomposite films more suitable for fruit and vegetable packaging and storage. However, this must be balanced with other important functional properties such as tensile and permeability properties.

All the films had slight greenish and yellowish color tinge. The greenness, yellowness, and the total color change increased significantly ($p<0.05$) while lightness reduced with BAH content. This is probably due to the greenish yellow color of the BAH nanoparticles used. Also, very high correlations were found between the optical properties for the nanocomposite films (r=0.978–1.000). Increased b^* correlated with reduced transparency while the reverse is the case with a^*.

Apart from the influence of constituent molecules on the optical properties, the surface finish is also important as it affects the light scattering effect and could ultimately affect the color perception and display properties such as glossiness and surface clarity of the films (Villalobos et al. 2005). Figure 2 shows the influence of BAH content on the surface characteristics of nanocomposite films using scanning electron microscope. It is evident that increased BAH content caused reduced surface finish and smoothness due to patches, crack, and holes formed at microscopic scale. The 3D topography as shown in Fig. 3 further confirms this. This explains why the transparency of the films decreased significantly ($p<0.05$) with BAH content.

Higher film clarity and surface finish are required for wrapping or covering display side of fresh fruit and vegetable boxes. The low biodegradability of synthetic plastics is partly

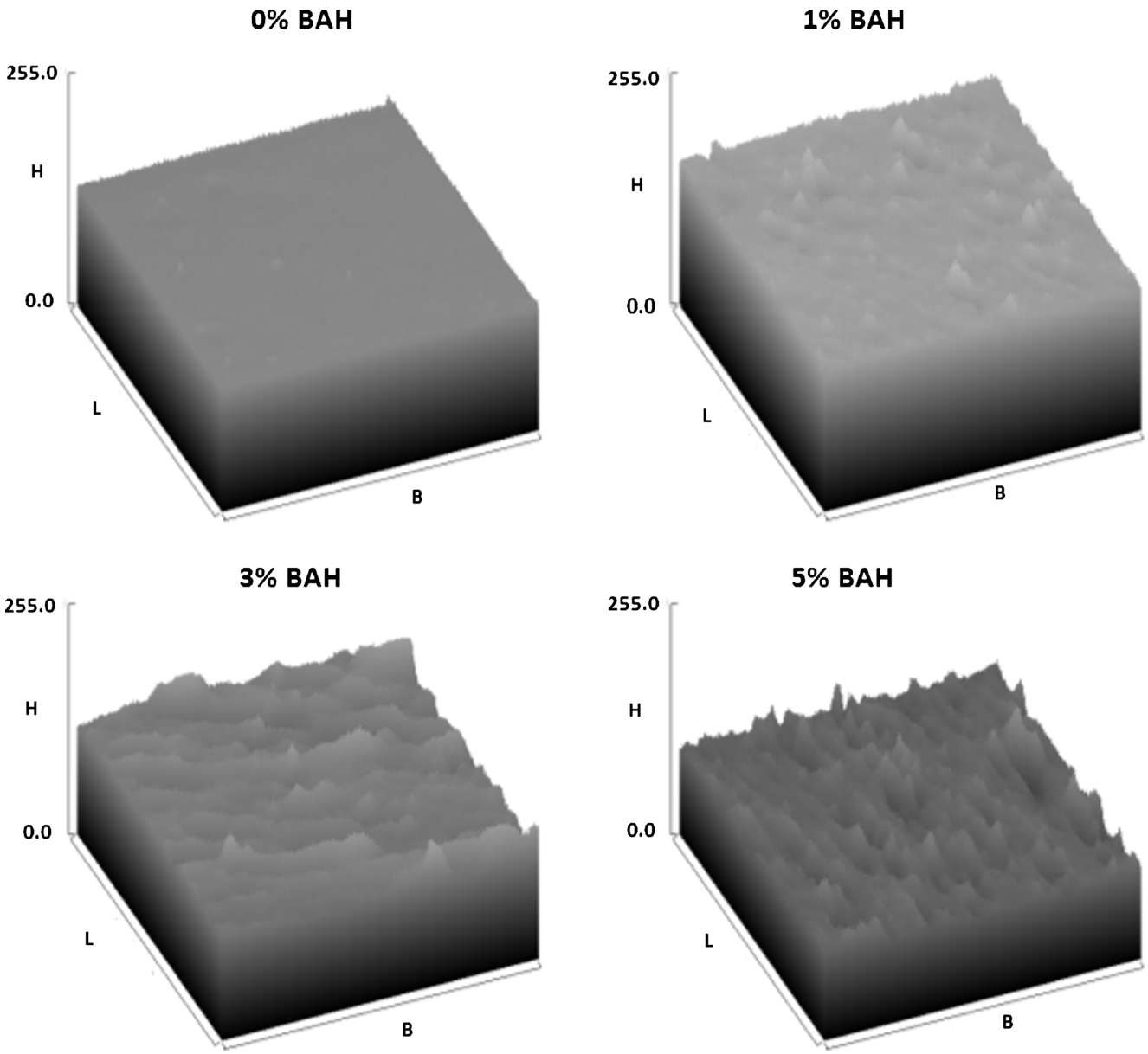

Fig. 3 3D plots of the gray value distribution showing the impact of BAH concentration on the surface finish of the chitosan-based films [The original image length (L) is 300 pixels and breadth (B) is 280 pixels and magnification of ×2,000].

due to their smoother surface that reduces adherence and attack of microbial cells while in contact with the soil (Aminabhavi et al. 1990). The reducing surface finish with higher BAH content observed in this study may imply increase susceptibility of the films to biodegradation when in contact with soil. This further suggests that the biodegradability of the films needs to be tested. Therefore, the reducing surface finish and transparency of the new composite film needs to be optimized against other functional properties affected by BAH content.

Knowing the effect of temperature on the water vapor permeability (WVP) of packaging film is in practice very useful as it will provide typical behavior and applicability of the material in normal usage. Such information about

Table 2 Water vapor permeability (10^{-10} g/Pa/s/m) of chitosan-based nanocomposite films as affected by BAH content and temperature

BAH content (%)	Temperature (°C)		
	12	22	35
0	17.06 (2.73)^{a}	12.74 (1.44)^{abc}	6.58 (1.47)^{d}
1	17.76 (0.14)^{a}	13.24 (1.61)^{abc}	7.49 (1.75)^{d}
3	17.25 (2.19)^{a}	12.63 (0.86)^{abc}	6.72 (1.16)^{d}
5	15.04 (4.33)^{ab}	11.19 (3.26)^{bcd}	8.41 (1.61)^{cd}

Means (n=2) followed by the same letter are not significantly different at $p<0.05$

Table 3 Parameters of Arrhenius model for the chitosan-based films loaded with BAH nanoparticles

BAH content (%)	E_a (kJ/mol)	WVP_o (g/m/Pa)	R^2
0	−3.33	0.9988	0.9987
1	−3.26	0.9988	0.9998
3	−3.36	0.9988	0.9998
5	−2.08	0.9993	0.9800

chitosan-based films is scarce. Most of the previous authors considered only one temperature in their studies. The WVP values which ranged between 6.58 and 17.76×10^{-10} g/m/s/Pa (Table 2) are quite higher than those reported by Cerqueira et al. (2012) for a chitosan-based packaging film. The compositional difference in the film forming solutions for these films could have created different microstructure which might be responsible for their different vapor permeability. The values are similar within the same temperature regardless of BAH content, but reduced linearly with increased air temperature. Condensability of water vapor increases with reduced temperature. As the condensability increases, swelling of hydrophilic polymers like chitosan tend to increase thereby creating more channels in the polymeric structure for free flow of vapor (Miranda et al., 2004). Thus, the increased WVP with lower temperature could be attributed to increase in molar free volume due to more extended molecular conformations of the solid matrix (Kerch and Korkhov 2011).

The Arrhenius plot of WVP with temperature gave very small but negative activation energy (E_a) values (Table 3). Similarly, small and negative E_a values have been reported by Auras et al. (2003) and Basha et al. (2011) for polylactide films. This observation firstly implies that water vapor transmission through the films is spontaneous as low energy change is required to permit the process. Negative E_a value is characteristic of a porous and low free volume glassy polymer membrane in which E_a of diffusion is smaller than that of sorption (Pinnau and Toy 1996). Another practical implication of this finding is that water vapor permeation would be enhanced at cold temperature as found in refrigerated food packaging applications. This could be of great advantage where reduced product dehydration and weight loss are needed such as in fresh fruits and vegetable packaging. However, in order to take advantage of this potential, air humidity outside the package should be constantly higher. Otherwise, the direction of water vapor diffusion will be reversed, i.e., water vapor will diffuse out of the package thereby leading to rapid product dehydration.

Table 4 Response surface regression parameters for predicting water vapor permeability of the chitosan-based films loaded with BAH nanoparticles

Terms	Coefficients	P value	Standard error
Constant	24.115	0.000	1.785
Temperature (°C) (T)	−0.557	0.013	0.161
BAH content (%) (B)	−0.380	0.459	0.481
T^2	0.002	0.648	0.003
B^2	−0.099	0.250	0.078
$T\times B$	0.031	0.032	0.012

The response of WVP to the influence of air temperature (Temp) and BAH content is shown by the surface plot (Fig. 4). The values of WVP could be predicted by a response surface regression model as follows:

$$\mathrm{WVP} = a_0 + a_1 * \mathrm{Temp} + a_2 * \mathrm{BAH} + a_3 * \mathrm{Temp}^2 + a_4 * \mathrm{BAH}^2 + a_5 * \mathrm{Temp} * \mathrm{BAH} \quad (9)$$

The regression parameters are shown in Table 4. It can be seen that WVP values are highly predictable given the high coefficient of determination (R^2=0.987) and low p value of 2.45E-05. It should be noted that the air temperature had significant effect on WVP value (p<0.05) unlike BAH content. However, the interaction between the two variables was significant on WVP value.

Table 1 shows the results of the tensile test performed on the films. The modulus of elasticity, elongation, and tensile strength

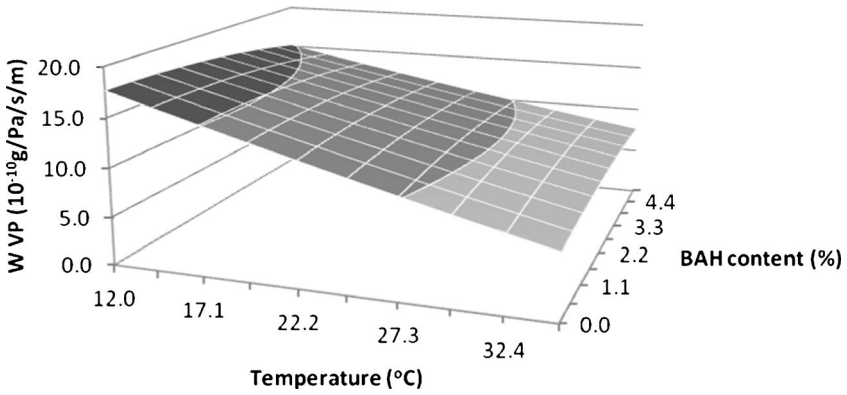

Fig. 4 Response surface plot of the effect of temperature and BAH content on the water vapor diffusion of the chitosan-based films

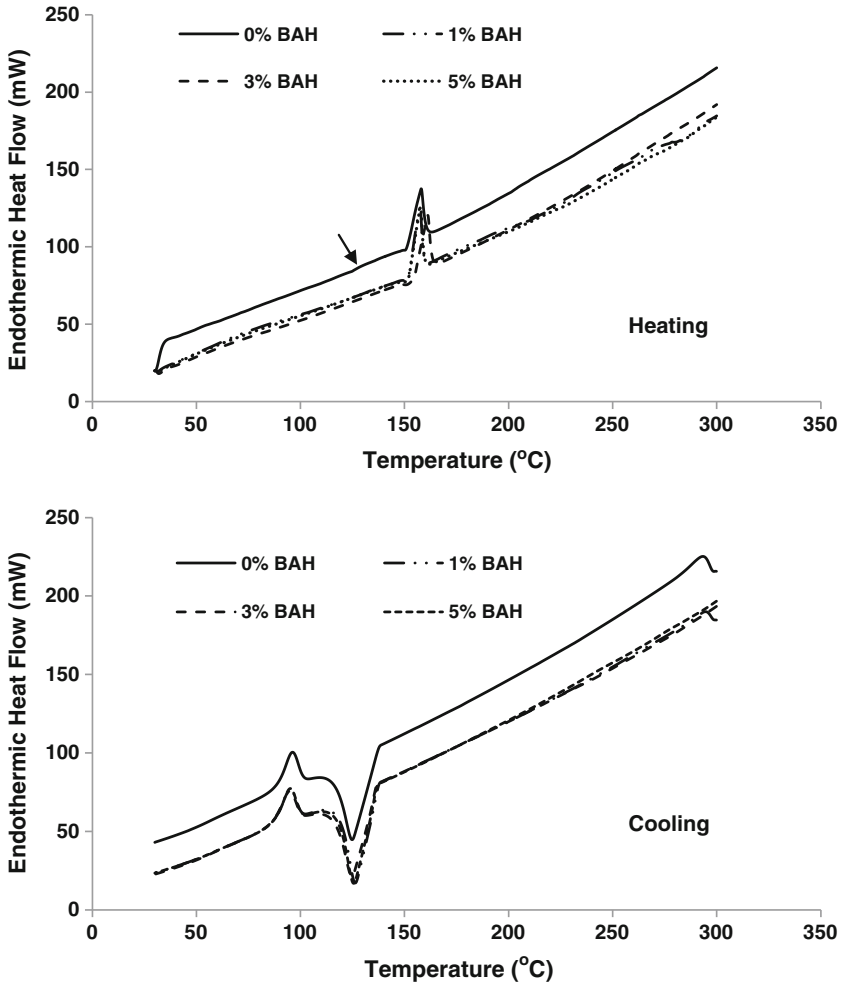

Fig. 5 DSC thermographs of the heating and cooling cycle of chitosan-based films at different BAH contents

ranged between 827.9 and 1097.1 MPa, 8.0 and 10.7 %, and 35.8 and 44.2 MPa, respectively. These values are similar to those reported by Srinivasa et al. (2007b) for neat chitosan films stored under different environmental conditions. Analysis of variance (ANOVA) showed that the mean values of the tensile properties of the chitosan films obtained during this study are not significantly different ($p>0.05$) in spite of the difference in BAH contents of the film. Mechanical properties of films are largely associated with distribution and density of intermolecular and intramolecular interactions in the network created in chitosan films (Leceta et al. 2013). This implies that the tensile properties of the films are similar and they would behave in the same manner when subjected to similar handling forces during use.

The thermal behavior of polymeric film determines the appropriate use and handling of the material. The thermal transition temperatures are indicative of the appropriate temperatures that must be used in sealing polymeric films and could be related to heat seal ability (Hernandez 1997). Low

Table 5 Thermal properties of chitosan-based nanocomposite films as affected by BAH loading

BAH content (%)	Heating cycle				Cooling cycle			
	T_o (°C)	T_p (°C)	ΔH_m (J/g)	T_p-T_o (°C)	T_o (°C)	T_p (°C)	ΔH_c (J/g)	T_p-T_o (°C)
0	151.9	157.5	1,028.8	5.6	137.6	126.5	902.6	11.1
1	151.4	158.0	1,055.5	6.6	137.7	125.2	901.9	12.5
3	154.6	161.2	1,054.1	6.6	136.6	124.5	935.5	12.1
5	152.0	157.7	1,041.4	5.7	136.8	125.7	941.5	11.1
Mean	152.5	158.6	1,045.0	6.1	137.2	125.5	920.4	11.7
Standard Deviation	1.4	1.7	12.5	0.6	0.6	0.8	21.1	0.7
CV %	0.9	1.1	1.2	9.0	0.4	0.7	2.3	6.1

melting and transition temperatures are needed for good sealing properties of plastic films. The heating and cooling curves as shown in Fig. 5 are important to completely project the thermal behavior of a polymeric film for different applications. The glass transition (T_g) marked by the sudden increase in enthalpy was observed only for the neat chitosan film at around 124.8 °C during the heating cycle. The unpronounced transition shown by the neat chitosan film indicates that it is near amorphous or semicrystalline in nature. However, the transition regions for the nanocomposite films are very inconspicuous and so it was difficult to determine the T_g from the curves. This could probably be due to its higher amorphous content following the inclusion of BAH nanofiller might have disrupted the crystalline layers of the matrix. Similar effect was observed by Honary et al. (2010) with inclusion of citrate in chitosan-based films. The single melting and cooling peaks observed indicate that the BAH addition did not have any pronounced effect on the thermal properties. The onset and peak of melting transition ranged between 151.4 and 154.6 °C and 157.5 and 161.2 °C, respectively (Table 5). The T_p values are higher than those reported for polyethylene and lower than those for pure polypropylene (Cho et al. 1999), which are the commonest synthetic polymers used in food packaging film production. The peak temperature and enthalpy of melting slightly increased with the addition of BAH. The recrystallization of the films during cooling cycle took place over a wider temperature range than melting during heating by two folds. Considering the coefficient of variation of the mean values of the parameters (Table 5), it can be concluded that the thermal behavior of the films are not significantly different, and as such, their sealing behavior may not be too different.

Conclusions

This study has shown that the inclusion of BAH nanoparticles in chitosan film caused significant differences in some physicochemical, optical, and barrier properties of the newly developed nanocomposite films. However, the thermal and tensile properties of the films were similar. The density, solubility, and water vapor permeability were highly predictable using linear, exponential, and full quadratic equations, respectively. The evaluated functional properties of the films suggest that they could be useful for fresh fruit and vegetable packaging. However, a separate experiment is therefore required to optimize the performance of the nanocomposite films for specific food packaging applications.

Acknowledgments This work was supported by a grant from the Post-Harvest Innovation Programme (Fresh Produce Exporter Forum, South Africa and Department of Science and Technology). The postdoctoral fellowship award provided for Dr. Taofik Akinyemi Shittu by the Directorate of Research & Innovation, Tshwane University of Technology, Pretoria, South Africa is gratefully acknowledged.

References

Abdollahi, M., Rezaei, M., & Farzi, G. (2012). A novel active bionanocomposite film incorporating rosemary essential oil and nanoclay into chitosan. *Journal of Food Engineering, 111*, 343–350.

Aminabhavi, T. M., Balundgi, R. H., & Cassidy, P. E. (1990). Review on biodegradable plastics. *Polymer Plastics Technology and Engineering, 29*(3), 235–262.

Amitava M., Mohammed S. I., Prathna T.C., & Chandrasekaran, N. (2011). Antimicrobial activity of aluminium oxide nanoparticles for potential clinical applications. In: Science against microbial pathogens: communicating current research and technological advances, A. Méndez-Vila (Ed.) Available at http://www.formatex.info/microbiology3/book/245-251.pdf

ASTM. (2009). *Standard test method for transparency of plastic sheeting*. Philadelphia: American Society for Testing and Materials.

ASTM. (1995). Standard test methods for tensile properties of thin plastic sheeting. In *Annual book of ASTM standards* (pp. 159–167). Philadelphia: American Society for Testing and Materials.

ASTM. (2008a). *Standard test method for temperature calibration of differential scanning calorimeters and differential thermal analyzers*. Philadelphia: American Society for Testing and Materials.

ASTM. (2008b). *Standard practice for heat flow calibration of differential scanning calorimeters*. Philadelphia: American Society for Testing and Materials.

Auras, R. A., Harte, B., Selke, S., & Hernandez, R. (2003). Mechanical, physical and barrier properties of polylactide films. *Journal of Plastic Film and Sheeting, 19*, 123–135.

Avella, M., Bruno, G., Errico, M. E., Gentile, G., Piciocchi, N., Sorrentino, A., et al. (2007). Innovative packaging for minimally processed fruits. *Packaging Technology and Science, 20*, 325–335.

Bajpai, S. K., Chand, N., & Chaurasia, V. (2012). Nano zinc oxide-loaded calcium alginate films with potential antibacterial properties. *Food and Bioprocess Technology, 5*(5), 1871–1881.

Bakhshi, D., & Arakawa, O. (2006). Induction of phenolic compounds biosynthesis with light irradiation in the flesh of red and yellow apples. *Journal of Applied Horticulture, 8*, 101–104.

Basha, R. K., Konno, K., Kani, H., & Kimura, T. (2011). Water vapor transmission rate of biomass based film materials. *Engineering in Agriculture, Environment and Food, 4*(2), 37–42.

Begin, A., & Van Calsteren, M. R. (1999). Antimicrobial films produced from chitosan. *International Journal of Biological Macromolecule, 26*, 63–67.

Bhunia, K., Dhawan, S., & Sablani, S. S. (2012). Modeling the oxygen diffusion of nanocomposite-based food packaging films. *Journal of Food Science, 77*(7), N29–N38.

Bourtoom, T., & Chinnan, M. S. (2008). Preparation and properties of rice starch-chitosan blend biodegradable film. *LWT-Food Science and Technology, 41*(9), 1633–1641.

Butler, B. L., Vergano, P. J., Testin, R. F., Bunn, J. M., & Wiles, J. L. (1996). Mechanical and barrier properties of edible chitosan films as affected by composition and storage. *Journal of Food Science, 61*(5), 952–955.

Caner, H., Hasipoglu, H., Yilmaz, O., & Yilmaz, E. (1998). Graft copolymerization of 4-vinylpyridine on to chitosan. I. By ceric ion initiation. *European Polymer Journal, 34*, 493–497.

Cerqueira, M. A., Souza, B. W. S., Teixeira, J. A., & Vicente, A. A. (2012). Effects of interactions between the constituents of chitosan-

edible films on their physical properties. *Food and Bioprocess Technology, 5*, 3181–3192.

Chen, Q., Tan, J. G. H., Liu, Y. C., Ng, W. K., & Zeng, X. T. (2008). Effect of boehmite nanorods on the properties of glycidoxypropyltrimethoxysilane (GPTS) hybrid coatings. *SIMTech Technical Reports, 9*(3), 154–160.

Cho, K., Li, F., & Choi, J. (1999). Crystallization and melting behavior of polypropylene and maleated polypropylene blends. *Polymer, 40*, 1719–1729.

Emamifar, A., Kadivar, M., Shahedi, M., & Solaimanianzad, S. (2010). Evaluation of nanocomposite packaging containing Ag and ZnO on the shelf life of fresh orange juice. *Innovative Food Science & Emerging Technologies, 11*(4), 742–748.

Forney, C. F., & Brandl, D. G. (1992). Small controlled environment chambers using glycerol-water solutions. *HortTechnology, 2*(1), 52–54.

Ghanem, A., & Skonberg, D. (2002). Effect of preparation method on the capture and release of biologically active molecules in chitosan gel beads. *Journal of Applied Polymer Science, 84*, 405–413.

Hernandez, R. (1997). Polymer properties. In *The Wiley encyclopedia of packaging technology* (2nd ed., pp. 758–765). New York: Wiley.

Honary, S., Hoseinzadeh, B., & Shalchian, P. (2010). The effect of polymer molecular weight on citrate crosslinked chitosan films for site-specific delivery of a non-polar drug. *Tropical Journal of Pharmaceutical Research, 9*(6), 525–531.

Hirano, S., Nakahira, T., Nakagawa, M., & Kim, S. K. (1999). The preparation and applications of functional fibers from crab shell chitin. *Journal of Biotechnology, 70*, 373–377.

Kerch, G., & Korkhov, V. (2011). Effect of storage time and temperature on structure, mechanical and barrier properties of chitosan-based films. *European Food Research and Technology, 232*, 17–22.

Khan, A., Khan, R. A., Salmieri, S., Tien, C. L., Riedl, B., Bouchard, J., et al. (2012). Mechanical and barrier properties of nanocrystalline cellulose reinforced chitosan based nanocomposite films. *Carbohydrate Polymers, 90*, 1601–1608.

Kim, K. M., Son, J. H., Kim, S.-K., Weller, C. L., & Hanna, M. A. (2006). Properties of chitosan films as a function of pH and solvent type. *Journal of Food Science, 71*(3), 119–124.

Leceta, I., Guerrero, P., & de la Caba, K. (2013). Functional properties of chitosan-based films. *Carbohydrate Polymers, 93*, 339–346.

Mailley, S. C., Hyland, M., Mailley, P., McLaughlin, J. M., & McAdams, E. T. (2000). Electrochemical and structural characterizations of electrodeposited iridium oxide thin-film electrodes applied to neurostimulating electrical signal. *Materials Science and Engineering, 21*, 167–175.

Mchugh, T. H., Aujard, J. F., & Krochta, J. M. (1994). Plasticized whey protein edible films: water vapor permeability properties. *Journal of Food Science, 59*, 416–419.

Miranda, S. P., Garnica, O., Sagahon, V. L., & Cardenas, G. (2004). Water vapor permeability and mechanical properties of chitosan composite films. *Journal of the Chilean Chemical Society, 49*(2), 173–178.

Ogunniran, E. S., Sadiku, R., Ray, S. S., & Luruli, N. (2012). Effect of boehmite alumina nanofiller incorporation on the morphology and thermal properties of functionalized poly(propylene)/polyamide 12 blends. *Macromolecular Materials and Engineering, 297*, 237–248.

Park, S. Y., Marsh, K. S., & Rhim, J. W. (2002). Characteristics of different molecular weight chitosan films affected by the type of organic solvents. *Journal of Food Science, 76*, 194–197.

Pinnau, I., & Toy, L. G. (1996). Gas and vapor transport properties of amorphous perfluorinated copolymer membranes based on 2,2-bistrifluoromethyl-4,5-difluoro-1.3dioxole/tetrafluoroethylene. *Journal of Membrane Science, 109*, 125–133.

Rodrıguez, M., Oses, J., Ziani, K., & Mate, J. I. (2006). Combined effect of plasticizers and surfactants on the physical properties of starch based edible films. *Food Research International, 39*, 840–846.

Schutz, C., Sort, J., Bacsik, Z., Oliynyk, V., Pellicer, E., Fall, A., et al. (2012). Hard and transparent films formed by nanocellulose—TiO_2 nanoparticle hybrids. *PLoS ONE, 7*(10), e45828. Available at www.plosone.org.

Singh, K., Suri, R., & Tiwary, A. K. (2012). Chitosan film: crosslinking with EDTA modifies physicochemical and mechanical properties. *Journal of Material Science, 23*, 687–695.

Srinivasa, P. C., Ramesh, M. N., & Tharanathan, R. N. (2007a). Effect of plasticizers and fatty acids on mechanical and permeability characteristics of chitosan films. *Food Hydrocolloids, 21*, 1113–1122.

Srinivasa, P. C., Ravi, R., & Tharanathan, R. N. (2007b). Effect of storage conditions on the tensile properties of eco-friendly chitosan films by response surface methodology. *Journal of Food Engineering, 80*, 184–189.

Srinivasa, P. C., Ramesh, M. N., Kumar, K. R., & Tharanathan, R. N. (2004). Properties of chitosan films prepared under different drying conditions. *Journal of Food Engineering, 63*, 79–85.

Stevens, E. S. (2003). What makes green plastics green? *Biocycle, 44*(3), 24–27.

Subramanian, P. M. (2000). Plastics recycling and waste management in the US. *Conservation and Recycling, 28*, 253–263.

Swapna, J. C., Harish, P. K. V., Rastogi, N. K., Indiramma, A. R., Yella, R. S., & Raghavarao, K. S. M. S. (2011). Optimum blend of chitosan and poly-(ε-caprolactone) for fabrication of films for food packaging applications. *Food and Bioprocess Technology, 4*, 1179–1185.

Tayel, A. A., El-Tras, W. F., Moussa, S., El-Baz, A. F., Mahrous, H., Salem, M. F., et al. (2011). Antibacterial action of zinc oxide nanoparticles against foodborne pathogens. *Journal of Food Safety, 31*(2), 211–218.

Tripathi, S., Mehtrotra, G. K., & Dutta, P. K. (2011). Chitosan–silver oxide nanocomposite film: preparation and antimicrobial activity. *Bulletin of Material Science, 34*, 29–35.

Ulbricht, M. (2006). Advanced functional polymer membranes. *Polymer, 47*, 2217–2262.

Villalobos, R., Chanona, J., Hernandez, P., Gutierrez, G., & Chiralt, A. (2005). Gloss and transparency of hydroxypropyl methylcellulose films containing surfactants as affected by their microstructure. *Food Hydrocolloids, 19*, 53–61.

Xu, H. X., Chen, J. W., & Xie, M. (2010). Effect of different light transmittance paper bags on fruit quality and antioxidant capacity in loquat. *Journal of the Science of Food and Agriculture, 90*, 1783–1788.

Zivanovic, S., Li, J., Davidson, P. M., & Kit, K. (2007). Physical, mechanical, and antibacterial properties of chitosan/PEO blend films. *Biomacromolecules, 8*, 1505–1510.